Brain Topogr (2015) 28:305–317
DOI 10.1007/s10548-014-0370-x

ORIGINAL PAPER

Detecting Functional Hubs of Ictogenic Networks

Frederic Zubler · Heidemarie Gast · Eugenio Abela · Christian Rummel · Martinus Hauf · Roland Wiest · Claudio Pollo · Kaspar Schindler

Received: 21 September 2013 / Accepted: 23 April 2014 / Published online: 21 May 2014

Abstract Quantitative EEG (qEEG) has modified our understanding of epileptic seizures, shifting our view from the traditionally accepted hyper-synchrony paradigm toward more complex models based on re-organization of functional networks. However, qEEG measurements are so far rarely considered during the clinical decision-making process. To better understand the dynamics of intracranial EEG signals, we examine a functional network derived from the quantification of information flow between intracranial EEG signals. Using transfer entropy, we analyzed 198 seizures from 27 patients undergoing pre-surgical evaluation for pharmaco-resistant epilepsy. During each seizure we considered for each network the in-, out- and total "hubs", defined respectively as the time and the EEG channels with the maximal incoming, outgoing or total (bidirectional) information flow. In the majority of cases we found that the hubs occur around the middle of seizures, and interestingly not at the beginning or end, where the most dramatic EEG signal changes are found by visual inspection. For the patients who then underwent surgery, good postoperative clinical outcome was on average associated with a higher percentage of out- or total-hubs located in the resected area (for out-hubs $p = 0.01$, for total-hubs $p = 0.04$). The location of in-hubs showed no clear predictive value. We conclude that the study of functional networks based on qEEG measurements may help to identify brain areas that are critical for seizure generation and are thus potential targets for focused therapeutic interventions.

Keywords Quantitative EEG · Functional brain networks · Epilepsy surgery · Symbolic transfer entropy

Introduction

While epilepsy has traditionally been associated with "hypersynchony" of neural activity (Penfield and Jasper 1954), more recent studies indicate that mechanisms of ictogenesis are more complex, in particular concerning the role of synchonization (Jiruska et al. 2013). Epilepsy is nowadays rather conceptualized as a disturbance in functional network (Kramer and Cash 2012; Engel et al. 2013; van Diessen et al. 2013). Networks can be mathematically represented as graphs, namely as set of nodes connected by edges. Networks in neuroscience have been defined based on anatomical data (the nodes representing brain areas, the edges anatomical connections), or based on functional studies such as fMRI or EEG (here the nodes representing voxels or EEG signals, and the edges some functional interdependence such as cross-correlation) (Schindler et al. 2008; Rubinov and Sporns 2010; He et al. 2011; Lemieux

Claudio Pollo and Kaspar Schindler shared last authorship.

Electronic supplementary material The online version of this article (doi:10.1007/s10548-014-0370-x) contains supplementary material, which is available to authorized users.

F. Zubler (✉) · H. Gast · K. Schindler
Department of Neurology, Inselspital Bern, Bern University Hospital, University of Bern, Bern, Switzerland
e-mail: frederic.zubler@gmail.com

E. Abela · C. Rummel · M. Hauf · R. Wiest
Support center for advanced Neuroimaging (SCAN), University Institute of Diagnostic and Interventional Neuroradiology, Inselspital Bern, Bern University Hospital, University of Bern, Bern, Switzerland

C. Pollo
Department of Neurosurgery, Inselspital Bern, Bern University Hospital, University of Bern, Bern, Switzerland

et al. 2011; Stam and van Straaten 2012). In the context of clinical epileptology, the hope is that identifying critical nodes of functional networks derived from electrophysiological signals will help us to identify those brain areas that are crucial for seizure generation. The ultimate goal is to refine and improve diagnostic and therapeutic methods for the many patients who are not seizure free despite treatment with seizure suppressive drugs.

In this paper we study functional networks derived from the quantification of information flow between intracranial EEG signals recorded in patients suffering from pharmacoresistant epilepsies and undergoing evaluation for possible epilepsy surgery. The method we use is based on transfer entropy (TE), a model-free information theoretic measure for quantifying the directed exchange of information between time series (Schreiber 2000). Compared to the well established Granger causality (Granger 1969), TE has the advantage to better detect non-linear relations. Unlike other proposed methods (Kaminski and Blinowska 1991; Wilke et al. 2008, 2011; Lizier et al. 2011; Lu et al. 2012) the original TE does not allow for multivariate signal analysis, but is easy to implement and computationally efficient.

Instead of applying TE directly to the raw signal value, we use symbolic transfer entropy (STE) (Staniek and Lehnertz 2008, 2009), whereby the TE is computed between symbolic transformations of the EEG signals (Daw et al. 2013; Zanin et al. 2012). The advantages of STE are first that it is computationally efficient, second that the procedure does not depend on the absolute amplitude of the signal, and thus is more robust to noise that is always present in real-world signals, and third, that the symbolization offers a natural binning for estimation of distributions and entropies (see "Methods" section).

After having computed the pairwise information flow between all EEG channels, we identify important nodes in the network as the ones with the maximal (over time and over all channels) incoming, outgoing, or total (i.e. bidirectional) information flow, which we refer to as hubs. We show that the three types of hubs typically occurred around the middle of the seizure, and that the location of the outgoing and total (but not of the incoming) hubs with respect to the resected brain area provide statistically significant information concerning the clinical outcome after epilepsy surgery.

Methods

Patients

For this retrospective study we included 27 consecutive patients (17 females) suffering from pharmacoresistant epilepsies who underwent long-term intracranial EEG monitoring (iEEG) at the department of Neurology of the University Hospital in Bern (Table 1). The mean age (± 1 standard deviation) was 30 ± 12 years (range 7–59 years). Except for the need for invasive EEG studies, there were no additional inclusion criteria. Specifically, patients with and without radiologically detectable lesions were enrolled. Retrospective data analysis had been approved by the Ethics Committee of the Kanton of Bern. In addition, all the patients gave written informed consent that their data from long-term video-EEG recordings might be used for research or teaching purposes.

EEG Recordings

As previously described (Schindler et al. 2011, 2012) EEG signals were recorded with intracranial strip, grid, or depth electrodes all manufactured by AD-TECH, Racine, WI, USA, with an extracranial reference electrode placed over the anterior sagittal region. The distance between contacts on a strip, grid, or depth electrodes was 1 cm. We used a NicoletOne recording system with a C64 amplifier (VIASYS Healthcare, Inc., Madison, WI, USA). The C64 contains AD7716 (Analog Devices, Inc., Norwood, MA, USA) sigma delta analog digital converters (ADCs) with modulator sampling frequencies of 570 kHz and amplitude resolutions of 16 bits. At the Nyquist frequency of 285 kHz, a one-pole low-pass filter with a corner frequency of 590 Hz provides 54 dB of attenuation before conversion. For the maximally possible sampling rate of 1,024 Hz, a digital low-pass (anti-aliasing) decimation filter within the ADC further attenuates the signal by 16 dB at 512 Hz. Signal analysis was done with MATLAB Version R2009a (MathWorks). EEG studies were either sampled at 512 or 1,024 Hz, depending on whether they were recorded with more or less than 64 electrodes.

All EEG signals were digitally band-pass filtered between 0.5 and 45 Hz (with a Butterworth filter of order 4) before analysis to avoid aliasing effects (see below). Forward and backward filtering was used in order to minimize phase distortions. Those EEG studies that had been recorded with a sampling rate of 1,024 Hz were then down sampled to 512 Hz prior to further analysis. EEG signals were referenced against the median of all the channels free of permanent artifacts as judged by visual inspection. EEG seizure onsets and endings were determined by the joint visual analysis of two experienced epileptologists (K.S. and H.G.). Seizures were excluded from analysis when the extracranially placed reference electrode was causing artifacts in all iEEG channels. In addition, seizure duration had to be longer than 10 s, but shorter than 30 min (in order to not fulfil the criteria for established status epilepticus) to be included for analysis.

Table 1 Patients information

No.	Gender	Age/ epilepsy duration (years)	Etiology	Outcome	SOZ	d[tot,out] (mm)	d[tot,in] (mm)	d[in,out] (mm)
1	F	25/19	Unknown	No seizure reduction	Amygdala right	26	65	59
2	F	19/16	Hippocampal sclerosis	Seizure free	Temporopolar/-lateral left	20	0	20
3	F	28/23	Hippocampal sclerosis	Seizure reduction	Bitemporal independent	0	0	0
4	M	36/20	Low-grade glioma	Seizure free	Temporolateral left	22	24	7
5	F	38/18	Dysplasia	Seizure reduction	Temporolateral left	0[a]	80[a]	80[a]
6	F	58/57	Hippocampal sclerosis	Seizure free	Temporopolar left	4	4	0
7	F	31/27	Tuberous sclerosis	No seizure reduction	Precentral right	0	35	35
8	M	27/7	Unknown	Seizure free	Temporomesial left	110	36	86
9	F	21/4	Meningitis	No seizure reduction	Temporopolar left	0[b]	28[b]	28[b]
10	F	27/4	Unknown	Seizure free	Temporomesial/-polar right	120[c]	116[c]	14[c]
11	F	27/7	Unknown	Seizure free	Temporoparietal right	28	47	23
12	M	24/4	Hippocampal sclerosis right	Seizure reduction	Temporal right	0	0	0
13	F	28/16	Ependymoblastom and traumatic head injury	Seizure reduction	Frontal left	0	14	14
14	M	18/14	Hippocampal sclerosis	Seizure free	Temporopolar right			
15	M	27/20	Clusters of dysplastic neurons	Seizure free	Temporolateral left			
16	M	31/27	Bilateral hippocampal sclerosis	Seizure reduction	Temporolateral left			
17	F	23/14	Cortical malformations	–	Bi-occipito-temporal			
18	M	28/19	Dysplasia left parietal lobe	–	Parietal left			
19	F	59/24	Suspected amygdala dysplasia	Seizure reduction	Temporopolar and frontal left			
20	M	26/18	Unknown	–	Bitemporal			
21	F	49/43	Cortical dysplasia	Seizure reduction	Frontal right			
22	M	31/20	Unknown	No seizure reduction	Temporo-parietal left			
23	F	56/49	Unknown	Seizure reduction	Temporolateral right			
24	M	20/5	Microdysgenesis type II	Seizure reduction	Amygdala right			
25	F	24/16	Unknown	Seizure free	Temporolateral left			
26	F	32/18	Meningitis	–	Temporal left			
27	F	7/7	Myelination defect / heterotopy	Seizure reduction	Temporal right			

SOZ, seizure onset zone defined by visual inspection; d[tot,out], euclidean distance between the position of the principal total-hub contact (that is, the electrode contact at which the signal was the most frequently the total-hub) and the principal out-hub contact; d[tot,in], euclidean distance between the position of the principal total-hub contact and the principal in-hub contact; d[in,out], euclidean distance between the position of the principal in-hub contact and the principal out-hub contact

a Principal total- and out-hub contact on the left hemisphere, principal in-hub contact on the right hemisphere

b Principal in-hub contact in white matter

c Principal total-hub contact on the left hemisphere, principal in- and out-hub contact on the right hemisphere

Bit Pattern Symbolic Transfer Entropy

We use symbolic transfer entropy (STE Staniek and Lehnertz 2008, 2009) to characterize the information flow between EEG signals. The method is illustrated in Fig. 1. Let x and y be the signals recorded at two EEG channels; in the following we denote x_t the value of signal x at time t. The first step in our analysis is to transform the original EEG signal into a bit string, that is a binary signal, which takes the value $b_t^x = 1$ if $x_t > x_{t-1}$ and 0 otherwise. We

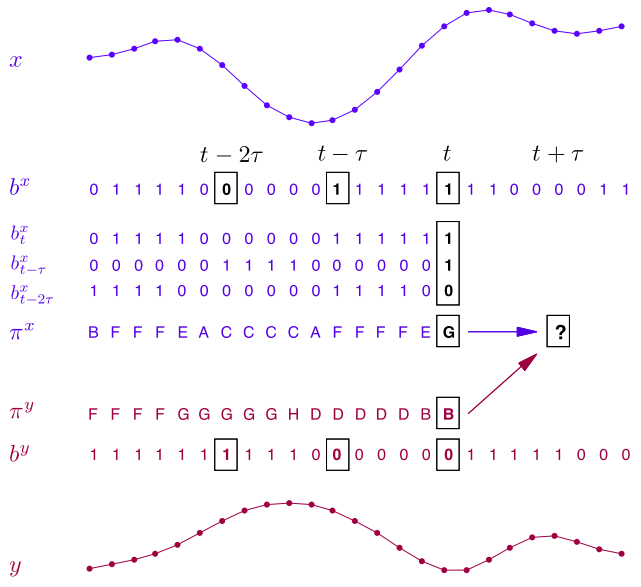

Fig. 1 Assessing information flow between two EEG signals with bit pattern symbolic transfer entropy. The EEG signals x and y are first transformed into bit strings (b^x, b^y), where a 0 represents a decrease or no change, and a 1 an increase in the amplitude of the original signal. A triplet of bits taken with a lag τ defines a *symbol*, which provides us with symbol strings π^x and π^y. The symbolic transfer entropy from y to x relates to the additional information on the future of π^x (knowing its current value) brought by the knowledge of the current value of π^y, expressed as the Kullback-Leibler divergence between $p(\pi^x_{t+\tau}|\pi^x_t)$ and $p(\pi^x_{t+\tau}|\pi^x_t, \pi^y_t)$

then define a symbol as a L-tuple of bits taken at an interval of τ time step(s). Because of the relatively short duration of the sampling window (see below) we restrict ourselves to the case $L = 3$. The analysis is performed with a time delay $\tau = 5$ sampling points, which is the largest possible value satisfying the condition $2\tau < T_{min}$, where T_{min} is the shortest period, i.e. one over the fastest frequency $(1/F_{max})$ in the filtered EEG signal. This condition is required to prevent aliasing problems (see Equations 4 and 5 in Rummel et al. 2013).

The symbolization procedure provides us with a string of symbols consisting of bit patterns $\pi^x_t = (b_t, b_{t-\tau}, b_{t-2\tau})$. For bit patterns of length 3, there are eight possible symbols $\{(0,0,0),(0,0,1),...,(1,1,1)\}$ (in Fig. 1 the different bit patterns are represented by the letters A-H). The symbolic transfer entropy from y to x, $ST(y \to x)$, corresponds to the transfer entropy between the corresponding strings of symbols $T(\pi^y \to \pi^x)$. It can be intuitively understood as a quantitative measure of the following procedure: assume we try to predict the future value of the symbolic transform of signal x based on the current symbol; how much better would we perform in our forecasting if we also took into account the current value of the symbolic transform of y. Mathematically, ST is expressed as the Kullback-Leibler divergence between the two conditional probability distributions $p(\pi^x_{t+h}|\pi^x_t)$ and $p(\pi^x_{t+h}|\pi^x_t, \pi^y_t)$. In this work we consider $h = \tau$, to avoid an additional parameter. Computing the symbolic transfer entropy between each ordered pair of EEG channels defines an asymmetrical matrix, that we interpret as a connectivity matrix defining a directed, weighted graph.

Practical Implementation and Correction Measures

We recall that if $p(\pi^x_t = i)$ denotes the probability for the symbol chain π^x to take the value i at time t, the Shannon entropy is $H(\pi^x_t) = \sum_i p(\pi^x_t = i)\log(p(\pi^x_t) = i)$, where the sum is taken over the 8 different symbols. Similarly, the joint entropy is $H(\pi^x_t, \pi^y_t) = \sum_{i,j} p(\pi^x_t = i, \pi^y_t = j)\log(p(\pi^x_t = i, \pi^y_t = j))$; for triplets the definition is analogous.

Following Kaiser and Schreiber (2002), the actual implementation of the transfer entropy between two symbol strings relies on the formulation of transfer entropy as a sum of four different block entropies: $T(\pi^y \to \pi^x) = H(\pi^x_t, \pi^x_{t+\tau}) + H(\pi^x_t, \pi^y_t) - H(\pi^x_t) - H(\pi^x_t, \pi^x_{t+\tau}, \pi^y_t)$. The probability distributions used for the computation of these entropies are empirically estimated by counting the relative occurrences of the different symbol combinations during a fixed time interval (since we use the same time lag $(\tau = h = 5)$ between the present and future symbol, and between the bits forming a symbol, there are respectively 2^4, 2^6, 2^3 and 2^7 different bits in the four block entropies mentioned earlier). The time window must be long enough to allow a reasonably accurate computation of the probability distributions, but it cannot be arbitrarily long because of the non-stationarity of the EEG signals during epileptic seizures. We use a sampling window of 2 s with a 1 s overlap, allowing each of the possible $2^7 = 128$ combinations of $p(\pi^x_t, \pi^x_{t+\tau}, \pi^y_t)$ to occur theoretically 8 times (in case of uniform distribution), while permitting a temporal resolution that allows to track the dynamic changes of periseizure EEG signals.

To correct for small sample effects we use a slightly modified version of the *effective transfer entropy* (ET) proposed by Marschinski and Kantz (2002): we compute 30 surrogate transfer entropies obtained using shuffled versions of π^y, the average of which is subtracted from the computed value: $ET(\pi^y \to \pi^x) = T(\pi^y \to \pi^x) - <T(\pi^y_{shuffled} \to \pi^x)>$; if this value is negative we take 0 instead, considering that no information flows from y to x. Finally we take an additional step suggested by Marschinski and Kantz in normalizing the amount of information transmitted from y to x by the information already contained in x. This defines the *relative explanation added* $REA = ET(\pi^y \to \pi^x)/H(\pi^x_t, \pi^x_{t+\tau})$.

Multimodal Coregistration

For safety reasons, the patients are not allowed into an MR scanner with intracranially implanted electrodes. The 13 more recently treated patients underwent pre- and postoperative magnetic resonance scans (MR_{pre} and MR_{post}, respectively) as well as stereotactic computer tomographies with high spatial resolution (CT_{stx}), allowing us to identify the location of intracranial EEG electrodes (Patients 1–13 in Table 1). To this end we use a multimodal coregistration procedure based on the high intensity metal artefacts visible on CT_{stx}. We use routines available in Statistical Parametric Mapping 8 (SPM8, http://www.fil.ion.ucl.ac.uk/spm/software/,r4667) and the Voxel-based Morphometry toolbox (VBM8, http://dbm.neuro.uni-jena.de/vbm/download/) running on MATLAB. All procedures are performed semiautomatically with custom made GUI-based batch files (http://sourceforge.net/apps/trac/matlabbatch/). First, CT_{stx} contrast is improved with a recently proposed ad hoc transformation (Rorden et al. 2012). The conversion from Hounsfield units (assuming the darkest voxel in the source image has an intensity of -1000) into arbitrary units (a.u.) is as follows: values -1000 to -100 are mapped to the range 0 to 900, values from -99 to 100 are linearly scaled to the range 901 to 3100, and values where $i > 100$ are set to the values $[i + 3000]$. These transformations provide sufficient contrast between skull, brain tissue and iEEG electrodes. Second, to improve coregistration, MR scans are denoised using a spatially adaptive non-local means filter. All images are manually realigned to the anterior commissure. A 6-parameter rigid-body coregistration (3 rotations, 3 translations) of MR_{post} to MR_{pre} is then computed by minimizing the normalized mutual information between both scans. These coregistration parameters are applied to CT_{stx}. Next, MR_{pre} is segmented into grey matter (GM), white matter (WM), cerebrospinal fluid (CSF) and non-brain tissue with SPM8's new segmentation routine; GM, WM and CSF are then recombined to form a skull-stripped brain image and a binary brain mask. CT_{stx} voxels that lay within this mask and above an intensity threshold $> 2,000$ a.u. are retained as electrodes.

Results

Identifying Hubs in STE Graphs

198 seizures from 27 patients were analyzed (on average 7.3 seizures/patient, range 2–29). The average duration of the seizures was 91 ± 105 s (range 10–1,001). On average 61 ± 17 channels (range 34–100) were recorded. As described in the "Methods" section, we used symbolic transfer entropy (STE) to characterize the information flow between each (ordered) pair of intracranial EEG channels, over a moving time window of 2 s with a 1 s overlap, during epileptic seizure and a pre- and post-ictal time period of 60 s. This procedure defines a graph, the nodes of which being the intracranial EEG signals, and the edges representing the information flow. This graph is thus directed and weighted, and evolves over time.

As a first step toward characterizing the properties of this graph we use the *degree-centrality*, i.e. we compute at each time step, and for each EEG channel, the in-degree (sum of all the weighted inputs to this node), the out-degree (sum of all the outputs) and the total degree (input degree plus output degree). In the following we define the *in-hub channel* (C_{in}), the *out-hub channel* (C_{out}), and the *total-hub channel* (C_{tot}) as the channels that attain respectively the maximal (in time and space) in-, out- or total degree. This definition for the hubs ensures that each seizure is associated with a single hub of each kind, and avoids arbitrary parameters (such as taking the n most highly connected nodes, or the top m percent). The time at which these maxima are reached are denoted *hub times* (t_{in}, t_{out}, and t_{tot}). Note that the different hubs might occur on the same channel and/or at the same time.

A typical example is demonstrated in Fig. 2. The first panel shows EEG signals at five different epochs in a 58 year old female with temporal lobe epilepsy (patient No. 6 in Table 1). For clarity we only display a subset of the channels, namely C_{tot} (channel DEL02) and the 10 channels that have the strongest total (i.e. input plus output) links to C_{tot}. For this particular seizure, we had $C_{tot} = C_{in} = C_{out}$, and $t_{tot} = t_{out}$, while the in-hub occurred 1 s later. The second and third panels show the connectivity matrix obtained by computing the information flow between each pair of nodes for the different epochs, and the resulting graph.

Figure 3a displays the sum of the incoming and outgoing information (i.e. the total degree in our graph) over time for all channels during the seizure shown in Fig. 2. There is a clear increase in information input and output a few seconds after seizure beginning, initially in the left depth electrode (channels 1–12) and in the left cortical temporo-polar strip electrode (channels 25–32), rapidly propagating to the other cortical electrodes on the left hemisphere (channels 41–46, 53–58). 54 s after seizure beginning, we observe propagation to the contralateral hemisphere. This sequence is so far consistent with the ictal patterns observed in the raw EEG signals. Searching for the global maximum, we find that C_{tot} is channel number 2 (second contact on the left depth temporal electrode), and $t_{tot} = 32$s. Thus, the total hub does not occur during one of the most salient changes of EEG signals (i.e. seizure beginning, propagation to the contralateral hemisphere or seizure termination), and thus cannot be

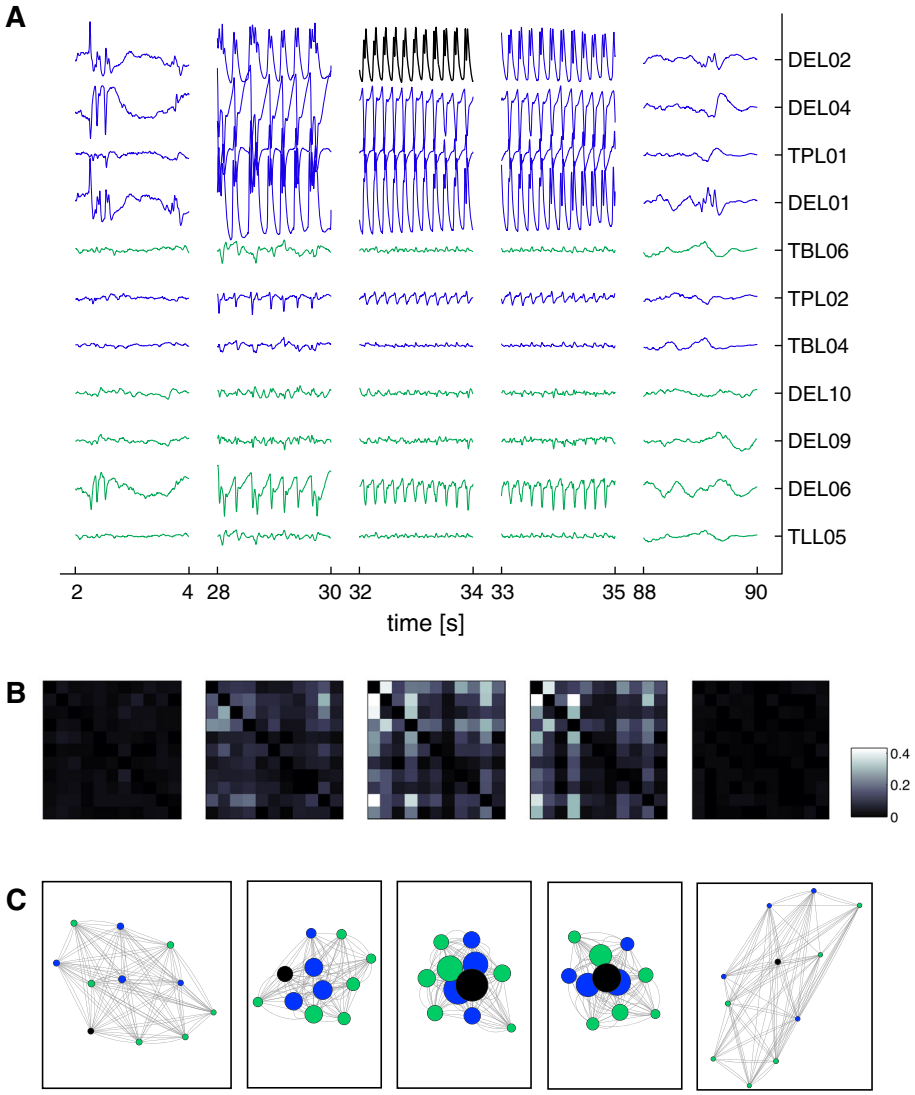

Fig. 2 **a** Ictal EEG recorded in a 58 year old female with temporal lobe epilepsy. Five epochs of 2 s are displayed, starting 2, 28, 32, 33 and 144 s after seizure onset. For clarity only 11 channels are shown. The topmost channel is the channel reaching the highest value of incoming, outgoing, and total information flow ($C_{in} = C_{out} = C_{tot} = \text{DEL02}$); the maximum outgoing and total flow occur during the third epoch ($t_{tot} = t_{out} = 32\text{s}$), while the maximum incoming information flow is reached during the fourth epoch (note the overlap between the third and fourth epoch). The other 10 channels are the ones that are the most strongly connected with the total-hub channel (as measured at t_{tot}). Color code: the total-hub is in *black*, the channels located in a brain region that was later removed during epilepsy surgery are in *blue*; the channels recorded in a brain region that was not removed are in *green*. **b** Value of symbolic transfer entropy (STE) computed between each ordered pair taken among the 11 electrodes, at the 5 epochs shown in (**a**), represented as matrices with $A_{ij} = \text{STE}(i \rightarrow j)$. **c** Graph obtained when the STE matrices are viewed as adjacency matrices. The nodes represent the EEG channels (the size of the node is proportional to the node total degree); the edges represent the STE between the signals recorded at each channel; on this representation the length of an edge is proportional to 1/log(STE). C_{tot} is in *black* in the five epochs; *blue* and *green* nodes represent respectively nodes that were removed and not removed. (Visualization with the Dynnetwork plug-in for the open-source program Cytoscape, http://code.google.com/p/dynnetwork) (Color figure online)

determined by visual inspection of the EEG signals. Furthermore, C_{tot} is not continuously the channel with the highest total degree (Fig. 3b), which indicates that this contact reaches the maximal value not uniquely because of the implantation schema. Figure 3d, e shows the degree over electrode and time for a 19 years old female suffering from an epilepsy with seizure onsets in the left mesial temporal brain regions (patient No. 2 in Table 1). In this patient electrodes were implanted only on the left hemisphere (Fig. 3f). C_{tot} was spatially less clearly delineated than in the previous patient, as many channels reach a high degree at about the same time. In this seizure $C_{tot} = C_{out}$,

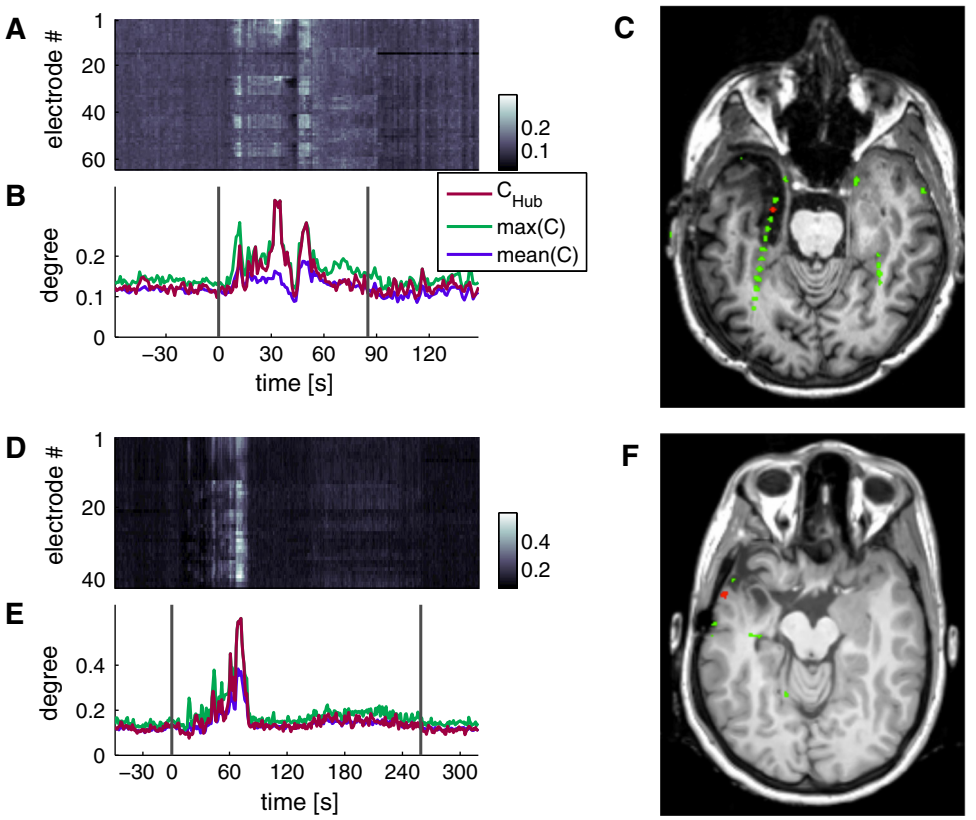

Fig. 3 **a** Periictal changes in total degree (sum of outgoing and incoming information flow) over time in the 64 channels recorded from a 58 years old female with TLE (same seizure as in Fig. 2). The maximum value over electrode and over space occurred 32 s after the visually determined seizure onset, in contact 2 of the deep electrode left (C_{tot}). **b** Evolution of the total degree of C_{tot} compared with the average degree over all channels (mean(C)) and the maximal degree at each epoch (max((C)). **c** Coregistered post operative MR showing the position of the electrodes for the patient considered in panels (**a**, **b**). The C_{tot} location (*red*) is in the resected region temporopolar left. **d**, **e** Periictal changes in the total degree in a 19 years old female with TLE. The total hub occurred 69 s after seizure onset, and was spatially less sharply circumscribed than was observed in the previous patient. **f** Axial MR showing the position of the electrodes. The C_{tot} location (*red*) is at the border of the resected area (Color figure online)

C_{in} being a different channel. All three hubs occurred at different time steps, but close to one another.

Averaged over all seizures, $C_{tot} = C_{in}$ in 33 % of the cases (64/198); $C_{tot} = C_{out}$ in 53 % (105/198), $C_{in} = C_{out}$ in only 18 % (36/198). We observed, though, that when not exactly on the same channels, the 3 different hubs often occurred on contacts in close vicinity. Besides, the exact concordance of the different hubs was further perturbed by the variability over different seizures within each patient. For instance we found that in the 17/27 patients who had at least 5 seizures, the average of the ratio (number of different total hubs)/(number of seizures) was 0.72 (range 0.11–1.0). This ratio might seem high, but the different C_{tot} were often clustered, as the total hubs occurred on average on 2.6 groups of channels (we call group all the channels on the same strip, the same depth electrode or the same grid; patients with at least 5 seizures had an average of 7.1 electrode groups per patients).

Characterizing t_{Hub}

In the two examples presented above, the hubs occurred in the middle or at the end of the first half of the seizures. To test if this finding is consistent in all patients, we analyzed the value of t_{tot}, t_{in}, and t_{out} in the 198 seizures considered. To allow for comparison between seizures of different durations, the ictal period was decomposed into 10 time bins of equal duration; in addition two pre (p) and two post (P) ictal bins of 30 s were included.

t_{tot} occurred during the ictal period in 76.6 % of the seizures, on average in the middle of the seizure, (mean ictal bin was 4.9; Fig. 4a). The timing tended to be consistent for multiple seizures within the same patient. For the 17/27 patients who had at least 5 seizures, the variance of bin number was 2.9 bins (range 0.45–5.62). A one-way ANOVA confirmed that the variability of bin between patients was larger than the variability within patients (p = 0.002). In most of the cases where t_{tot} occurred in the pre or

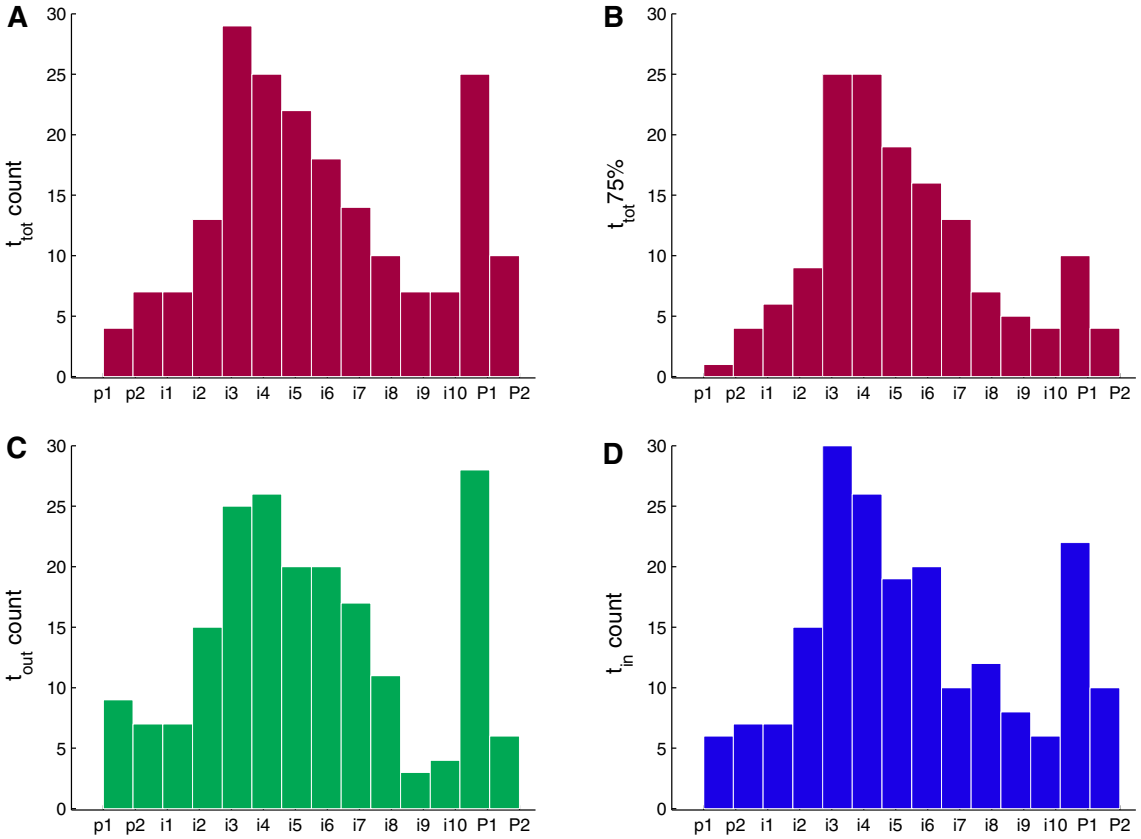

Fig. 4 Distribution of hub times. To allow for comparison between seizures of different durations, the ictal period was decomposed into 10 time bins of equal duration; in addition two pre (p) and two post (P) ictal bins of 30 s each were included. **a** Distribution of t_{tot} in all 198 seizures; the hubs occurred during the seizures in 156 cases (76.7 %), predominantly in the middle of the seizure. **b** when considering only the 75 % seizures with least interictal epileptiform activity, 87.2 % of the hubs occurred during the seizures. **c** Distribution of t_{out}. **d** Distribution of t_{in}

post-ictal time period, pronounced interictal epileptic discharges were present. This could be shown by computing the absolute slope of the EEG signal (before symbolization), which is a good indicator for epileptiform activity as it increases for high amplitude, but also for high frequency low amplitude signals (Schindler et al. 2007). We defined the interictal epileptiform activity as the average absolute slope over all channels, during 60 s before and 60 s after the seizure. Considering only the seizures below the 75th percentile of interictal activity, the proportion of total-hub occurring during the seizure reached 87 % (Fig. 4b). Comparing the hub times for the different hubs we found that $t_{tot} = t_{in}$ in 53 % of the seizures (106/198), and $t_{tot} = t_{out}$ in 61 %(121/198). Although not exactly equal, the three hub times followed a similar distribution (Fig. 4cd).

Figure 5 shows a summary of the degree-centrality increase leading to hub formation. The absolute values have been normalized (the total-hub degree being set to 1). $< C_{tot} >$ indicates a temporal average of the hub electrode over the consecutive 14 time bins, and a pooling over all seizures; $<< C >>$ indicates that the average has been taken twice, over the time periods and over all the electrodes. 17/198 seizures with durations of less than 20 s have been excluded to ensure that each time bin would be the average of at least two epochs. Both for $< C_{tot} >$ and $<< C >>$ the total degree increased during the first half of the seizures, and then decreased during the second half of the seizures, with a small deflection before seizure termination (Fig. 5a). If we examine separately the evolution over time of the incoming and the outgoing flow in total-hub channels, we see that the maximal outdegree occurred at the middle of the seizure for $<< C >>$, but interestingly for $< C_{tot} >$ the maximum was reached toward the end of the seizure (Fig. 5b); this effect was independent of seizure durations, that is the maximum of the outdegree in bin i9 was found consistently in seizure subgroups of duration <60 s, 60–120 s, 120–180 s and >180 s (results not displayed). On average the total incoming information exceeds the total outgoing information in total-hub channels. The median difference is maximum at the end of the first half of the seizure (bin i5), and the order of magnitude is around 5 % (see Fig. 5d; the difference output–input for

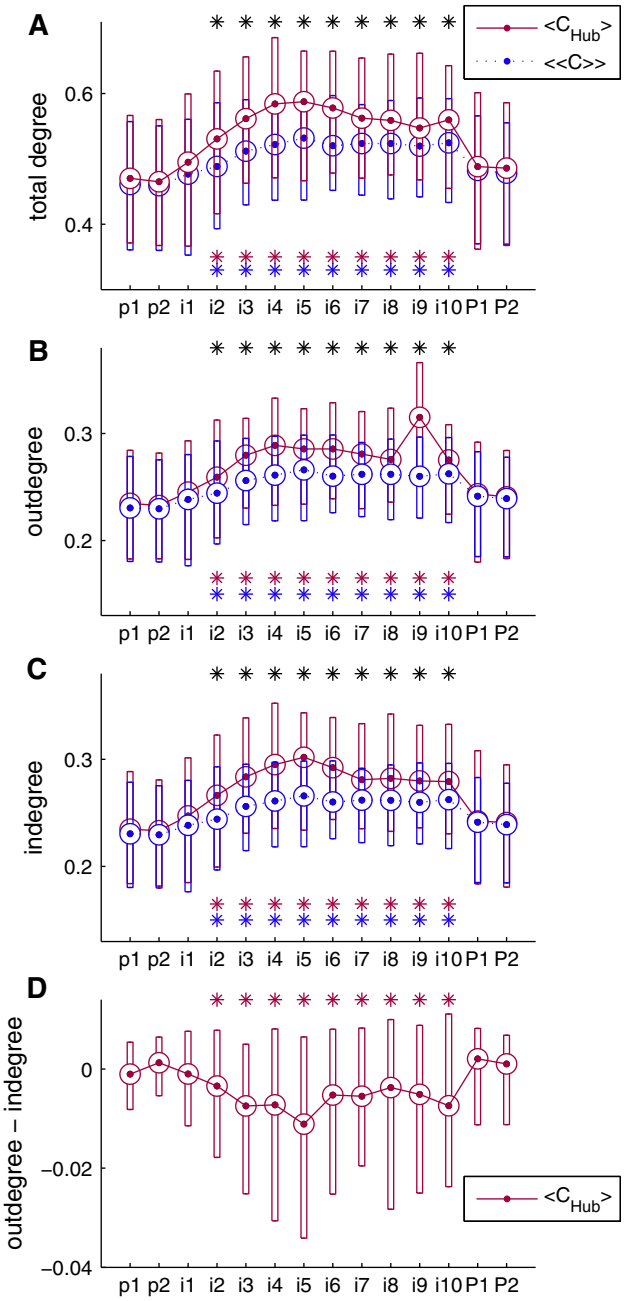

Fig. 5 **a** Summary plot showing the temporal evolution of the total degree in the total-hub channels ($<C_{tot}>$) and the average over all channels ($<<C>>$), averaged over 181 seizures lasting at least 20 s. Both measurements increase during the first half of the seizures, and decreases during the second half of the seizures. To allow for comparison between seizures of different durations, the ictal period was decomposed into 10 time bins of equal duration; in addition two pre (p) and two post (P) ictal bins of 30 s each were included. Bars represent the interquartile range and encircled bullets the median; the connecting line is for eye guidance only. *Colored asterisks* indicate statistically significant difference with bin p1; *black asterisks* indicate significant difference between the two measurements within one time bin (Wilcoxon–Mann–Whitney-test, Bonferroni correction for multiple comparisons). **b–d** Summary plot for the outdegree, the indegree and the difference output minus input in the $<C_{tot}>$ and in all other electrodes (Color figure online)

$<<C>>$ is not displayed as it is zero by definition). The results were very similar for the in-hubs and the out-hubs (supplementary Fig. 1). In particular, the median (over all patients) of the *output* degree (averaged over each time bin) was maximal in bin i9 in C_{in} and in C_{out} (even though the out-hub occurs predominantly in the middle of the seizure, as discussed above).

The temporal evolution in nodes degree described above resulted from weight modifications in existing links, and not from a change in the number of links, which did not significantly vary during the seizure (supplementary Figs. 2, 3) The concomitant increase in *node heterogeneity* (a measure of how spread the distribution of node degrees is Liu et al. 2011; supplementary Fig. 4) confirms that the ictal increase in information flow was not uniformly distributed, allowing for the emergence of hubs.

Predictive Value of C_{tot}, C_{in}, and C_{out} for Clinical Outcome

Should the different hub locations be targeted for epilepsy surgery? To answer this clinically highly relevant question we had the possibility to precisely identify with a coregistration method (see "Methods" section) the electrode locations in 13 patients. In particular we could determine which electrode channels had been implanted into a brain area that was later removed during surgery, and the clinical outcome could be compared with the removal of the different hubs. Since in the same patient different channels reached the maximal in-, out- or total degree for different seizures, we considered the percentage of these hubs removed, namely the number of seizure(s) for which the hub channel has been removed divided by the total number of seizures. Because of the relatively small number of patients, we subdivided the patients outcome into two categories: The first category consisted of patients who became completely seizure and aura free after the operation; this group contained six patients (46 %). The second category contained seven patients, three of them with reduction in seizure rate, and four others who unfortunately did not benefit from the intervention. On average, seizure-free patients had the total-hub removed in 50 % of their seizures (range 0–100 %), while only 15.8 % total-hub channels were removed in patients who were not seizure free (range 0–40 %). The observed difference between the two groups was statistically significant ($p = 0.038$, assessed with a non-parametric permutation test (Nichols and Holmes 2001)). It is interesting to note that while we found patients with a good outcome in whom no hub locations were removed, none of the patients with more than 40% hub removal had a persistence of seizures after surgery (Fig. 6a). Figure 3c shows the reconstructed electrode

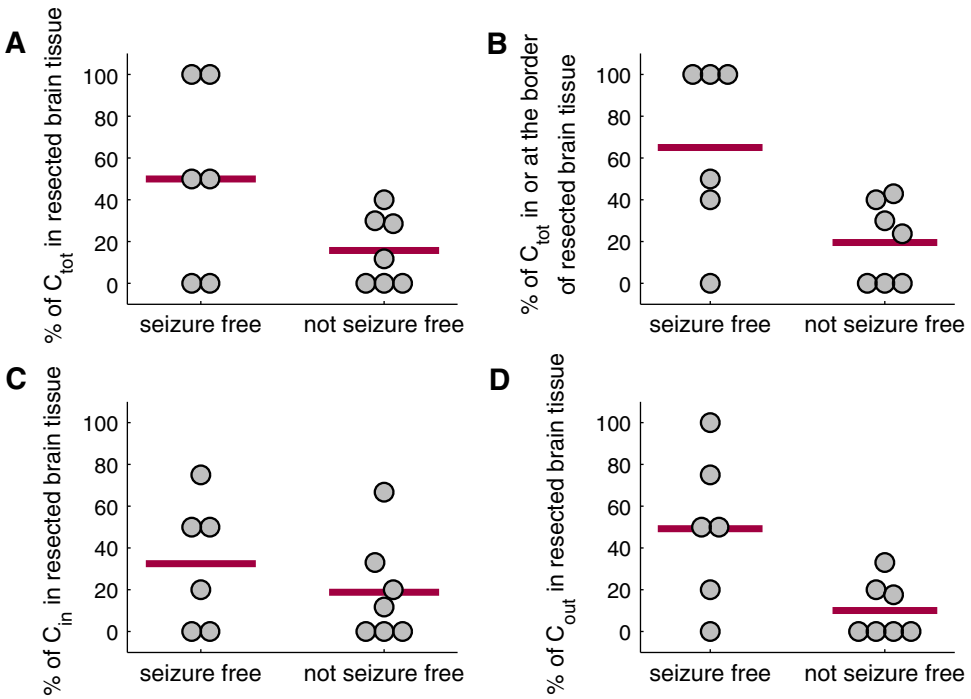

Fig. 6 **a** Relation between the resection of total-hubs' locations and clinical outcome. The percentage of C_{tot} located in a region that was later removed during epilepsy surgery was on average 50 % in patients who were seizure-free after the operation, and 15.8 % in patients who were not seizure free (p = 0.038, non parametric permutation test). No patient with more than 40 % total-hub locations resected continued to have seizures. **b** Taking the proximity to resection border into account: if we consider the total-hub channels that were either located in a region that was later removed, or that were direct neighbor with a channel that was later removed, we found an average percentage of 65 % in patients seizure free after intervention, and 19.5 % in patients not seizure free (p = 0.013). **c** The resection rate of channels reaching the maximum in-degree (C_{in}) was respectively 27.9 and 21.9 in the two groups of patients; the difference was not statistically significant (p = 0.34). **d** From the three types of hubs, the best predictive value was reached when considering the removal of channels with maximum out-degree (C_{out}), with in average of 49.1 % removal in seizure-free patients, and of 10.0 % in patients who were still symptomatic (p = 0.011)

location of C_{tot} in a patient with a good outcome after removal of the hub location.

In patients who became seizure free without resection of all the total-hubs, we observed sometimes that the C_{tot} location was immediately adjacent to the resection border (an example is shown in Fig. 3f). To quantify this phenomenon we considered all C_{tot} with a neighboring contact on the same electrode that had been removed. This definition is rather conservative, in that a hub channel geometrically close to the resected area, but with no adjacent contact in that area would not be taken into account. If we compare the percentage of hub channels removed or with removed neighbors in the two patient group we find a mean removal rate of 65 % in group 1 and of 19.5 % in group 2 (p = 0.013; Fig. 6b).

The same analysis was performed for in-hubs and out-hubs. As shown in Fig. 6c, the surgical removal of C_{in} correlated poorly with the clinical outcome (p = 0.19); in contrast, nodes with maximal out-degree had the highest predictive value from all types of hubs (mean C_{out} removal percentage in patients with good outcome = 49 %, in patients with not satisfactory outcome = 10.0 %, p = 0.011).

Alternative Hub Definitions

As previously mentioned, by focusing on the global maximum degree over time and channels we could avoid the introduction of arbitrary parameters in defining a hub. On the other hand, we often observed in patients who had different channels reaching the maximum in different seizures, that the hub channel in one seizure would reach the second or third largest degree in another seizure. We decided thus to test if taking into account three highly connected nodes might allow more robust clinical predictions. The combined removal percentage of the three channels reaching the highest total-degree (not necessarily at the same time) did yield a slightly better predictive value than for the removal of a single total-hub (the mean for seizure-free patients was 142 % (range 0–300), mean for not seizure-free patients was 48 % (range 0–158); p = 0.028).

Averaging the total-degree over the duration of the seizure—instead of considering the maximal value over time—did not clearly improve the correlation with post-surgical outcome (the removal percentage of channels with maximal averaged degree was 50 % (range 0–100) in seizure-free patients, and 19 % (range 0–70) in non seizure-free patients; $p = 0.19$).

Beside the *degree centrality* used above, other functions have been proposed to characterize the importance of the nodes in a graph. One of these alternative measures is *betweeness centrality* (BC), which has been previously shown to correlate with clinical outcome after epilepsy surgery in a functional network defined with directed transfer function (Wilke et al. 2011). For a given node k, BC is defined as the fraction of shortest (weighted) paths between all pairs of other nodes $(i \neq k, j \neq k)$ passing through k. Obviously, the BC changes over time with the modification of the functional graph. At t_{tot}, the node with highest BC was in 79 % of the seizures also the C_{tot}. The predictive value of the removal of node with highest BC was $p = 0.044$, that is, close to the p value obtained for the removal of C_{hub}. The nodes with highest BC one minute before seizure beginning and one minute after seizure termination corresponded to C_{hub} in only respectively 1.3 and 3.5 % of the seizures; their predictive value were $p = 0.08$ and 0.66.

Conclusion

We have studied the periictal evolution of functional networks derived from intracranial EEG signals and defined with bit pattern symbolic transfer entropy.

A consistent finding was the occurrence of the (temporal and spatial) maximal in-degree, out-degree and total-degree, which we called hub, predominantly in the middle of the seizure. Comparing the location of the channels reaching these global maxima with clinical outcome after epilepsy surgery, we have shown that removal of the total-hub channels or of one of its direct neighbors, or the removal of the out-hub channels has prognostic value. In particular, in our patient collective, no patient had a bad outcome (defined as persistence of aura or seizures) after removal of more than 40 % of the total hubs or more than 33 % of the out-hubs.

One possible interpretation of these results is that the hubs do play an active role (or at least a permissive role) in the course of a seizure. In this context, the dynamic of the ictal total degree, which increases more strongly at the hub nodes than at other nodes, and which most often decreases prior to seizure termination, would permit the initiation and the propagation of the seizure, and would have to decline to permit seizure termination. Interestingly, several properties measured in ictal functional networks have been shown to have the same temporal dynamics than hubs' degree centrality. For instance, Kramer et al. (2010) have shown that a network defined with cross-correlation becomes transiently more fragmented during a seizure, and re-connects before seizure termination. Schindler et al. (2007) have demonstrated an initial decrease, followed by an increase of synchrony as measured with multi-channel EEG correlation. Schindler et al. also demonstrated that a peak in *signal redundancy* (a local measure of variability derived from permutation entropy) occurs in the middle of the ictal phase (Schindler et al. 2012). At the single cell level, neuronal firing rate and inter-spike variability follow a similar dynamics, as observered by Truccolo et al. (2011). Obviously the hypothesis of a seizure promoting role of the hubs is also supported by the beneficial effect of hub resection, and especially the correlation between the predictive value of the hubs' removal and their output degree $(C_{out} > C_{tot} > C_{in})$.

A second, opposite interpretation of our results, in which the generation of the hubs help to terminate the seizure is also theoretically possible. Electroencephalographers have observed for decades how seizures often terminate simultaneously across many channels. More recently, this phenomenon has been studied at systems level (Kramer et al. 2012), and confirmed at single neuron level (Truccolo et al. 2011). In this context, the increase in outgoing information flow observed at the hub channels in the ictal bin i9 (Fig. 5b, Supplementary Fig. 1b) would represent the synchronisation signal sent throughout the network to stop the seizure. The trend between postoperative seizure reduction and hub resection does not entirely rule out this hypothesis, if the hub regions both initiate, and then help terminate the seizures (for instance if acting as a "synchronising region", since synchronisation seems to be present at seizure initiation, but then later also be necessary for seizure termination (Jiruska et al. 2013). This hypothesis might imply that patients in whom the (out- and total-) hubs are removed, and who still have seizures, could have longer seizures, or a higher risk of developing a status epilepticus; which has yet to be confirmed.

Finally, we note that the third interpretation, according to which the hubs are a mere consequence of the rise in collective behavior, is consistent neither with the probable benefit of total- and out-hubs' resection, nor with the dynamics of mutual information, which gradually increase during the seizure development, but without consecutive inflection of the curve before termination (Schindler et al. 2012).

The hubs are not always located in the seizure onset zone (SOZ; result not shown). Yet this does not rule out a postulated pro-ictogenic role of hubs in the early ictal phase. Indeed, the hubs could in certain cases be activated shortly after seizure begin, to promote seizure propagation. The latter would explain why the average incoming information to the hubs overweighs the outgoing

information, making the hubs (even the output-hub) on average driven, more than driving nodes. A positive outcome despite non-resection of any total-hubs as observed in 2/6 patients (Fig. 6a) would then be explained by the deafferentation of the hubs, depriving them from the necessary input permitting their formation and their seizure promoting effects. This hypothesis is indirectly supported by the high percentage of seizures in which C_{tot} was also the node with highest betweenness centrality (BC); and by the findings of Warren et al. (2010) showing that the correlation between electrodes inside and outside the SOZ was smaller than the correlation between pairs of electrodes both within or outside the SOZ (which was interpreted as a functional deconnection of the SOZ from other brain regions). Indeed, the BC is particularly high in nodes that connect disparate parts of a graph (Rubinov and Sporns 2010), making the hubs good candidates for being the "relay station" between the SOZ and the rest of the brain. (Note however that the work of Warren et al. was performed on interictal recordings; whereas we have observed that one minute before, or one minute after the seizure, the concordance between C_{tot} and nodes with maximal BC disappeared).

The results of our study may be clinically relevant. Indeed EEG analysis to determine target brain areas for resective or functional epilepsy surgery is still largely based on visual inspection, especially the identification of the seizure onset zone based on the presence of low amplitude fast oscillations or other epileptiform signals. In contrast, identifying the hub channel is based on quantitative signal analysis, which detects patterns that are not obvious in the raw EEG signals. Moreover, the spatial and temporal location of the hubs (not occurring during the beginning or the end of the seizure where the most dramatic EEG changes occur, and not in the seizure onset zone) makes it more likely to add additional insight in selecting the brain area to be resected, to the mere study of initial fast oscillations. Beside surgery, the hub locations could also be potential targets for therapeutical stimulations (Bondallaz et al. 2012). Further studies will be needed to better characterize functional ictal networks, in particular to explore new definitions and roles of hubs. It will be interesting to adopt a multi-scale approach, combining a bottom-up (how the hub influences the network in permitting seizure development) and a top- down (how, in turn, the global activity/large-scale patterns of the network influences the information flow through the hub) view. We expect that the study of EEG derived functional networks based on methods of graph theory will gain importance in the near future for the study of ictogenesis, and will eventually become a powerful aid for diagnostic and therapeutic procedures.

References

Bondallaz P, Box C, Rossetti AO, Foletti G, Spinelli L, Vulliemoz S, Seeck M, Pollo C (2012) Electrode location and clinical outcome in hippocampal electrical stimulation for mesial temporal lobe epilepsy. Seizure 13:1059–1311

Daw CS, Finney CEA, Tracy ER (2013) A review of symbolic analysis of experimental data. Rev Sci Instrum 74:915–930

Engel J, Thompson PM, Stern JM, Staba RJ, Bragin A, Mody I (2013) Connectomics and epilepsy. Curr Opin Neurol 26(2):186–194

Granger CWJ (1969) Investigating causal relations by econometric models and cross-spectral methods. Econometrica 37(3):424–438

He B, Yang L, Wilke C, Yuan H (2011) Electrophysiological imaging of brain activity and connectivity-challenges and opportunities. IEEE Trans Biomed Eng 58(7):1918–31

Jiruska P, de Curtis M, Jefferys JGR, Schevon CA, Schiff SJ, Schindler K (2013) Synchronization and desynchronization in epilepsy: controversies and hypotheses. J Physiol 591(4):787–97

Kaiser A, Schreiber T (2002) Information transfer in continuous processes. Phys D 166(1):43–62

Kaminski MJ, Blinowska KJ (1991) A new method of the description of the information flow in the brain structures. Biol Cybern 65:203–210

Kramer MA, Eden UT, Kolaczyk ED, Zepeda R, Eskandar EN, Cash SS (2010) Coalescence and fragmentation of cortical networks during focal seizures. J Neurosci 30:10076–10085

Kramer MA, Cash SS (2012) Epilepsy as a disorder of cortical network organization. Neuroscientist 18(4):360–372

Kramer MA, Truccolo W, Eden UT, Lepage KQ, Hochberg LR, Eskandar EN, Madsen JR, Lee JW, Maheshwari A, Halgren E, Chu CJ, Cash SS (2012) Human seizures self-terminate across spatial scales via a critical transitino. Proc Natl Acad Sci 09(51):21116–21

Lemieux L, Daunizeau J, Walker MC (2011) Concepts of connectivity and human epileptic activity. Front Syst Neurosci 5:12

Liu YY, Slotine JJ, Barabsi AL (2011) Controlability of complex networks. Nature 473:167–173

Lizier JT, Heinzle J, Horstmann A, Haynes JD, Prokopenko M (2011) Multivariate information-theoretic measures reveal directed information structure and task relevant changes in fMRI connectivity. J Comput Neurosci 30(1):85–107

Lu Y, Yang L, Worrell GA, He B (2012) Seizure source imaging by means of FINE spatio-temporal dipole localization and directed transfer function in partial epilepsy patients. Clin Neurophysiol 123(7):1275–1283

Marschinski R, Kantz H (2002) Analysing the information flow between financial time series. Eur Phys J B 3(2):275–281

Nichols TE, Holmes AP (2001) Nonparametric permutation tests for functional neuroimaging: a primer with examples. Hum Brain Mapp 15:1–25

Penfield W, Jasper H (1954) Epilepsy and the functional anatomy of the human brain. Little Brown, Boston

Rorden C, Bonilha L, Fridriksson J, Bender B, Karnath HO (2012) Age-specific CT and MRI templates for spatial normalization. Neuroimage 61(4):957–965

Rubinov M, Sporns O (2010) Complex network measures of brain connectivity: uses and interpretations. Neuroimage 52(3):1059–1069

Rummel C, Abela E, Hauf M, Wiest R, Schindler K (2013) Ordinal patterns in epileptic brains: analysis of intracranial EEG and simultaneous EEG-fMRI. Eur Phys J Spec Top 222:569–585

Schindler K, Leung H, Elger CE, Lehnertz K (2007) Assessing seizure dynamics by analyzing the correlation structure of multichannel intracranial EEG. Brain 130:65–77

Schindler K, Bialonski S, Horstmann MT, Elger CE, Lehnertz K (2008) Evolving functional network properties and synchronizability during human epileptic seizures. Chaos 18:033119

Schindler K, Gast H, Stieglitz L, Stibal A, Hauf M, Wiest R, Mariani L, Rummel C (2011) Forbidden ordinal patterns of periictal intracranial EEG indicate deterministic dynamics in human epileptic seizures. Epilepsia 52(10):1771–1780

Schindler K, Gast H, Goodfellow M, Rummel C (2012) On seeing the trees and the forest: single-signal and multisignal analysis of periictal intracranial EEG. Epilepsia 53(9):1658–1668

Schreiber T (2000) Measuring information transfer. Phys Rev Lett 85:461–464

Stam CJ, van Straaten ECW (2012) The organization of physiological brain networks. Clin Neurophysiol 123(6):1067–1087

Staniek M, Lehnertz K (2008) Symbolic transfer entropy. Phys Rev Lett 100(15):158101

Staniek M, Lehnertz K (2009) Symbolic transfer entropy: inferring directionality in biosignals. Biomed Tech 54(6):323–328

Truccolo W, Donoghue JA, Hochberg LR, Eskandar EN, Madsen JR, Anderson WS, Brown EN, Halgren E, Cash SS (2011) Single-neuron dynamics in human focal epilepsy. Nat Neurosc 14:635–641

van Diessen E, Diederen SJH, Braun KPJ, Jansen FE, Stam CJ (2013) Functional and structural brain networks in epilepsy: what have we learned? Epilepsia 54(11):1855–1865

Warren CP, Hu S, Stead M, Brinkmann BH, Bower MR, Worrell GA (2010) Synchrony in normal and focal epileptic brain: the seizure onset zone is functionally disconnected. J Neurophysiol 104(6): 3530–3539

Wilke C, Ding L, He B (2008) Estimation of time-varying connectivity patterns through the use of an adaptive directed transfer function. IEEE Trans Biomed Eng 55(11):2557–2564

Wilke C, Worrell G, He B (2011) Graph analysis of epileptogenic networks in human partial epilepsy. Epilepsia 52(1):84–93

Zanin M, Zunino L, Rosso OA, Papo D (2012) Permutation entropy and its main biomedical and econophysics applications: a review. Entropy 14(8):1553–1577